MIC2022
22nd Machining Innovations Conference for Aerospace Industry

Proceedings are available on SSRN: www.ssrn.com

SSRN Proceedings Hosted on SSRN.com

MIC Procedia (2022) 051–058

22nd Machining Innovations Conference for Aerospace Industry 2022 (MIC 2022), November 30th and December 1st 2022, Hannover, Germany

Machinability analysis for milling of additively manufactured Inconel 718 with specifically induced porosity

S. A. M. Schneider[a,*], S. Hermsen[b], S. Kirchmann[a], P. Ganser[a], T. Bergs[a], J. H. Schleifenbaum[b]

[a]*Fraunhofer Institute for Production Technology IPT, Steinbachstrasse 17, 52074 Aachen, Germany*
[b]*Chair for Digital Additive Production DAP of RWTH Aachen University, Campus-Boulevard 73, 52074 Aachen, Germany*

* Corresponding author. Tel.: +49 241 8904-398. *E-mail address:* sebastian.schneider@ipt.fraunhofer.de

Abstract

Compared to conventional manufacturing technologies, additive manufacturing (AM) offers great design freedom, the integration of functions into components, new lightweight construction concepts and high material efficiency. This technology is increasingly coming into focus in aerospace and turbomachinery engineering, especially the Laser Powder Bed Fusion (LPBF) process. LPBF is already being used for some aerospace components that are often subject to high thermal and mechanical loads. Depending on the component geometry, support structures are required for additive manufacturing, which then have to be removed, usually by machining. Among others, the use of material with specifically induced porosity is suitable as a support structure. This ensures good heat dissipation and thus homogeneous component properties, high retention forces and short process times in the LPBF process. However, the machinability of porous, additively manufactured material has hardly been researched to date. This paper therefore presents the results of machinability investigations with porous, additively manufactured Inconel 718. The investigations included the analysis of active cutting force, cutting tool wear, surface finish and chip geometry in the milling process with tungsten carbide cutting tools. It was found that with the porous material, the dominant type of wear is early starting chipping of the cutting tool edges. The active force decreases with increasing porosity. Partial smearing of the pores was observed on the milled surfaces. The chips of the porous material show a disrupted surface. In future investigations, the aim is to improve the wear behaviour when milling porous Inconel 718.

© 2022 The Authors. Published by SSRN, available online at https://www.ssrn.com/link/MIC-2022.html
This is an open access article under the CC BY-NC-ND license (http://creativecommons.org/licenses/by-nc-nd/4.0/)
Peer review statement: Peer-review under responsibility of the scientific committee of the 22nd Machining Innovations Conference for Aerospace Industry 2022

Keywords: LPBF; SLM; additive manufacturing; AM; porous; porosity; Inconel 718; alloy 718; milling; support structure

1. Introduction and State of the Art

Compared to conventional manufacturing technologies, additive manufacturing (AM) offers several advantages, such as great design freedom, integration of functions into components, new lightweight concepts and high material efficiency. AM is increasingly coming into focus in aerospace and turbomachinery engineering, especially the Laser Powder Bed Fusion (LPBF) process. LPBF is already being used for some aerospace components that are often subject to high thermal and mechanical loads [1]. Depending on the component geometry, support structures are required for additive manufacturing, which then have to be removed, usually by machining. Among others, the use of material with specifically induced porosity is suitable as a support structure. In the context of this paper, porous material with a relative density ≥ 72 % is considered. Compared to conventional AM support structures, like block supports, a porous volume support ensures good heat dissipation and thus homogeneous component properties, high retention forces and short process times in the LPBF process. However, the machinability of porous, additively manufactured material has hardly been researched to date. Inconel 718

© 2022 The Authors. Published by SSRN, available online at https://www.ssrn.com/link/MIC-2022.html
This is an open access article under the CC BY-NC-ND license (http://creativecommons.org/licenses/by-nc-nd/4.0/)
Peer review statement: Peer-review under responsibility of the scientific committee of the 22nd Machining Innovations Conference for Aerospace Industry 2022.

Electronic copy available at: https://ssrn.com/abstract=4259357

(IN718) is the most widely used and most researched material among the high-temperature nickel alloys, which are often applied for turbomachinery applications. For this reason, this paper presents the results of machinability studies in milling porous AM IN718 with different relative densities (100 %, 84 %, 72 %) respectively porosities (0 %, 16 %, 28 %).

According to DIN8580 [2], AM processes are classified as primary forming processes since three-dimensional components are produced automatically from shapeless or shape-neutral starting material. Characteristics are the element- or layer-wise build-up from the starting material or the phase transition of the material from powdery or liquid to solid as differentiation to the material-removing subtractive processes [3,4]. LPBF, also known as Selective Laser Melting (SLM), is a commonly used AM process with metal powder as feedstock and three repetitive steps to manufacture the final shape, or near final shape parts. This is accomplished by layer-wise selective melting of metal powder with a laser as an energy source [5]. The LPBF process can be split up into three steps:

1) Preprocessing: The 3D model of the part is designed and sliced in layers of a constant thickness (typically 0.01 – 0.1 mm) and corresponding scanning vectors are assigned in each layer. Additionally, the LPBF machine is prepared by installing and aligning a substrate plate. Afterwards, the sieved metal powder is filled into the LPBF machine.

2) Processing: The processing itself can be divided into the three following sub-steps which are performed for each layer until the part is finished: a) Coating an even and homogenous layer of metal powder on the substrate or previous layer with the recoating system. b) Selective melting and fusion through the scanning laser in accordance with the geometric information of the specific layer which connects the layer with the previous one. c) Lowering the platform by the layer thickness. The whole processing is performed in an inert gas atmosphere which is circulating through a filter system to prevent oxidation of the heated metal [5,6].

3) Postprocessing: After the building process, the remaining metal powder is removed from the part, which is afterwards detached from the LPBF machine and substrate plate. If necessary, support structures are removed, and a surface or heat treatment may be performed as well.

The main process parameters of the LPBF control the energy input during manufacturing and therefore strongly influence the quality of the manufactured part. Especially part density, surface condition and dimensional accuracy are influenced by the energy input and therefore by the LPBF process parameters: Laser power P_L, scanning speed v_s, hatch spacing Δy_s and layer thickness D_s. These LPBF process parameters are schematically shown in Fig. 1. The scanning speed refers to the velocity of the laser beam passing the scanning vectors which are defined during slicing. The hatch spacing is the distance between two scanning vectors. With increasing layer thickness, the number of layers for a part decreases, which increases the build-up rate. Regardless, higher layer thicknesses decrease the part quality and dimensional accuracy especially in arch-shaped parts. Furthermore, the preferable energy input depends on the processed material as well as on the economic trade-off between large build-up rate, part quality and dimensional accuracy [5,7,8].

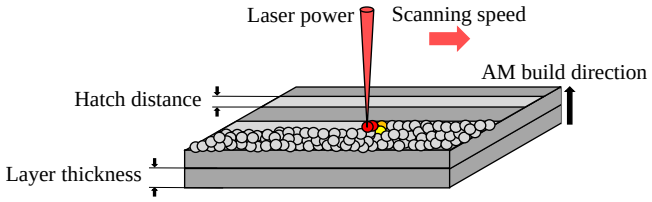

Fig. 1. Process parameters in LPBF [4,9]

Support structures required in the LPBF process must be removed after the component has been manufactured and heat treated. In some cases, manual removal is sufficient, but only if the material and the required support structure geometry allow it. Additive manufacturing usually cannot achieve the necessary dimensional accuracy or surface qualities of demanding components, so subtractive finishing is necessary. It therefore makes sense to remove the support structures automatically as part of the subtractive finishing process.

Milling is a metal-cutting manufacturing process with a circular cutting motion of a usually multi-toothed tool to produce any workpiece surface. The cutting movement is perpendicular or oblique to the tool's axis of rotation [10]. Milling is one of the cutting processes that are defined in DIN 8589 [11]. In general, cutting processes are divided into roughing and finishing. While in the roughing process the aim is to achieve the highest possible metal removal rate, the finishing process aims to machine the largest possible surface area while taking into account the requirements for the surface to be produced [12]. The removal of support structures is therefore a roughing process, with the aim of removing the support structures as quickly or as economically as possible. In order to quantitatively evaluate and compare machining processes, different machinability criteria exist. Typical machinability criteria are the cutting force, the cutting tool life, the surface quality or the chip form [10]. An evaluation of the surface quality is particularly used for finishing processes but may also be interesting for roughing processes for betting process understanding.

In this paper, the material Inconel 718 (IN718) is investigated. This is a nickel alloy which is used, for example, in aircraft turbines or stationary gas turbines. Nickel alloys are materials with nickel as the main component alloyed with at least one other element. They are characterized by good corrosion resistance and/or excellent high-temperature strength [10]. IN718 is the most widely used and most researched material among the high-temperature nickel alloys due to its excellent chemical and physical properties at high temperatures. However, the material properties of IN718 also result in very poor machinability, particularly due to the following characteristics: high strength under elevated temperatures, high hardness, high strength of the material, high degree of work hardening, poor thermal conductivity and high tendency of built-up edge. The dominant wear mechanisms are adhesion wear, abrasive wear, diffusion wear, oxidation wear and debonding failure [13].

Electronic copy available at: https://ssrn.com/abstract=4259357

For conventional applications, IN718 is used in the cast or wrought stage. In this paper, however, a material manufactured additively in the LPBF process is investigated. The material properties and also the machinability of AM IN718 differ from the conventional material. Generally, the properties of AM IN718 strongly depend on the AM technique, the AM process parameters and strategy and the heat treatment. However, Hosseini et al. [14] were able to extract some general statements in their literature review. The hardness and the tensile strength of AM IN718 are typically between those of the cast and wrought material. AM-induced defects and poor surface quality usually lead to lower fatigue performance than wrought IN718 but some process optimizations show even higher fatigue strength. In comparison to the conventional material, AM IN718 shows anisotropy in mechanical properties when comparing the AM build direction with the other directions. Typically, higher elastic modulus and tensile strength, longer constant-stress-amplitude fatigue endurance, shorter constant-strain-amplitude fatigue endurance and shorter creep rupture time can be observed perpendicular to the build direction [14].

The differences between AM and conventional IN718 also influence machinability. The AM material shows smaller dimension of TiC and NbC carbides compared to the wrought material which may lead to reduced abrasive tool wear. The anisotropy of material properties leads to anisotropy in machining. Thus, the feed direction has a significant influence on machinability. Besides, AM IN718 indicates more fluctuation of thermo-mechanical loads on the cutting tool so cutting tools with higher toughness are beneficial [15]. For process design, it must be considered that the optimum process parameters may be different for machining AM and conventional IN718. A clear tendency regarding tool wear cannot be identified, since the properties of AM IN718 depend strongly on the individual AM process and heat treatment [16].

This paper compares the machinability of solid and porous AM IN718. Based on the literature, significant differences are to be expected. Valdez et al. [17] investigated the properties of AM IN718 with induced porosity between 1 and 30 %. Their results showed a strong decrease of tensile strength, elongation, compressive yield strength and elastic modulus with increasing porosity [17]. However, due to the wide range of settings possible in the LPBF process, the porosity specification does not allow any conclusions to be drawn about the exact structure of the AM component, but only indicates the ratio between the void and total volume of the component.

Hardly any relevant publications could be found on the machinability in macro milling of additively manufactured material, comparable to the porous material used in this investigation, with specifically induced porosity up to 28 %, particularly not for IN718. Some publications deal with the influence of the undesired porosity on machining that occurs in the LPBF process. Wood et al. [18], for example, investigated the turning of porous IN718 produced in the LPBF process, but only up to a porosity of 3 %. Kelliger et al. [28] investigated the machinability of AM 316L with 3.2 % porosity. However, if powder metallurgically (PM) produced material is considered, there are several publications on the machinability of porous material. In general, sintered porous material exhibits significantly poorer machinability compared to the corresponding solid material. In addition, lower cutting forces but higher tool wear are observed. This is in contrast to the general observation for solid materials that tool wear also increases with higher cutting forces [19].

Different theories exist to explain the mechanisms involved in the machining of porous material. Tutunea-Fatan et al. [19] and Salak et al. [20] point out two contradicting theories in particular. The 'interrupted cutting theory' tries to explain the increased tool wear with the frequent entry and exit of individual cutting edge areas in the porous material and the resulting high mechanical alternating load. This is said to cause microfractures and also stronger vibrations, which strongly accelerate tool wear. The second theory is the ‘deformation cutting theory’, which is based on the formation of a work-hardened layer in the rim zone. This hardened layer is created by plastic flow processes in which the material is pressed into the pores during the machining process and partially closes them. This effect is also called 'porosity closure phenomenon', i.e. the smearing of the pores in the surface layer by the machining process [19]. According to [19] and [20], the two described theories contradict each other in the case where the deformation of the porous PM material and the closing of the pores cause the cutting tool edge to cut compacted, ‘solid’ material and the machinability then depends only on the properties of this compacted material. In this case, machinability of the porous PM material may be even better. Another theory is the ‘thermal conductivity theory’ [20-22]. It explains the poor machinability with the thermal conductivity which decreases linearly with increasing porosity [23]. As the thermal conductivity decreases, less heat can be transferred from the cutting zone and, thus, thermal based tool wear effects become more severe [22].

In general, several of the described mechanisms act simultaneously and the extent to which they contribute to the machinability of the porous material depends very much on the application [20]. It is reasonable to assume that the mechanisms observed in the machining of porous PM material also apply in principle to porous AM material, albeit certainly to different extents. In this paper, the results of milling trials with porous AM IN718 are presented and subsequently analysed and discussed.

2. AM Inconel 718 with specifically induced porosity

MetcoAdd™ 718C powder from OC Oerlikon Corporation AG was used for processing the LPBF samples. The powder was produced by vacuum melting and gas atomization under argon. The material batch with a particle size D50 of 38.1 µm (D10 = 29.9 µm, D90 = 43.4 µm) was characterized by spherical particles with isolated satellites. The particles also had a high relative density and showed only isolated pores. The LPBF samples were manufactured on an EOS M290 system by EOS GmbH, with a building chamber building size of 250 x 250 x 325 mm³. The beam source of the machine is a single-

Electronic copy available at: https://ssrn.com/abstract=4259357

mode fibre laser with a wavelength of 1064 nm and a maximum power output of 400 W. The scan vectors were rotated by 33.3° per layer and a stripe pattern with a stripe width of 5 mm was applied. For the validation and characterization of the porous structure cuboid samples with dimensions of 10 x 10 x 10 mm³ were manufactured. To determine the level and stability of the induced porosity the samples were investigated metallographically, parallel as well as perpendicular to the build direction. The mechanical properties of the structures were investigated with tensile tests. Cylindrical rods with a diameter of 6 mm and a height of 60 mm were manufactured in parallel and perpendicular to AM build direction. The tensile tests were conducted by TPW Prüfzentrum GmbH in accordance with ISO 6892-1:2009 (B) [24]. The results of the tensile strength R_m at room temperature are shown in Table 1.

For the milling trials additionally cuboid samples with the dimensions of 40 x 40 x 40 mm³ were manufactured. All samples were manufactured on a C45 substrate plate. Process parameter sets to achieve the desired relative densities were determined in earlier experiments. After metallographic analysis, three parameter sets with different achieved relative densities were selected for the trials (Table 1).

Table 1. LPBF process and material properties of the investigated samples

No.	Laser power [W]	Scanning speed [mm/s]	Hatch distance [µm]	Layer thickness [µm]	**Relative density [%]**	Tensile Strength = [MPa]	Tensile Strength ⊥ [MPa]	LPBF Time [%]
A	285	960	120	40	≈ **100**	1504	1576	100
B	285	960	200	80	≈ **84**	585	814	30
C	370	1500	220	80	≈ **72**	291	415	20

'=' : parallel to AM build direction, '⊥' : perpendicular to AM build direction

Selected micrographs of cross sections are shown in Fig. 2. The cross sections are shown perpendicular and parallel to the LPBF build direction. The goal was to achieve a uniform distributed structure with a low process time which allows the use as a support structure. In order to adjust the mechanical properties a heat treatment of the produced samples was applied. The heat treatment was performed by Oetzbach Edelstahl GmbH according to the AMS 5663 standard.

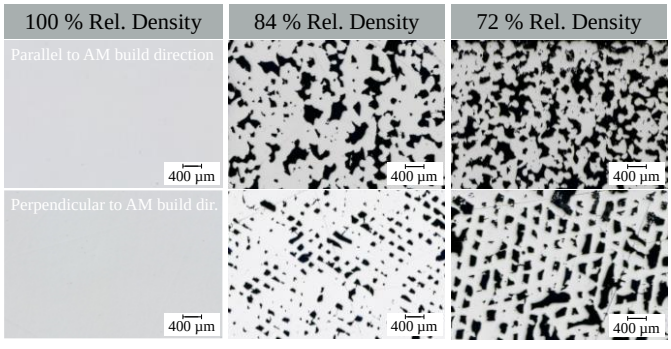

Fig. 2. Micrographs of material sample cross sections

3. Experimental Setup and Test Plan

The experimental setup for the milling trials is shown in Fig. 3. The trials were carried out on a Makino D500 five-axis-milling machine. The cutting tool was clamped in a Regofix holder using the HSK63 interface. The test samples with dimensions 40 x 40 x 40 mm³ were fixed with the help of a vice. The vice was clamped on a Kistler 9255B multi-component dynamometer which was mounted on the machine table.

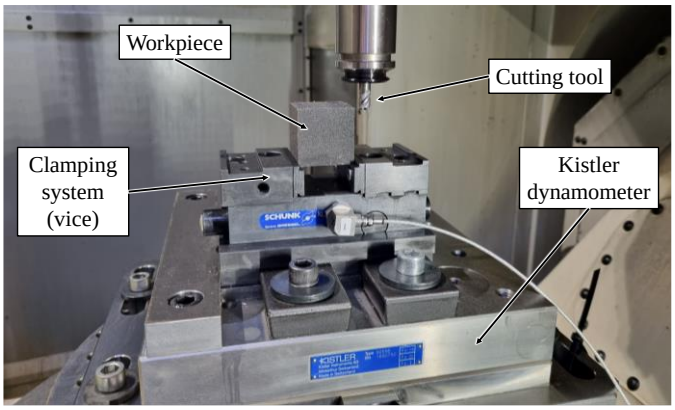

Fig. 3. Experimental setup for milling trials

The milling tools were carbide end mills with corner radius made by Präwest Präzisionswerkstätten Dr.-Ing. Heinz-Rudolf Jung GmbH & Co. KG. The tools with four cutting edges had a diameter of D = 8 mm, a corner radius of r = 1.5 mm and a helix angle of λ = 38°. The cutting material was uncoated tungsten carbide with a cobalt content of 10 % and a grain size of 0.7 µm. The cutting edges were prepared and showed an average cutting edge radius of 9.2 µm. Regarding the workpiece material used in the trials all information can be found in section 2 of this paper. A partial factorial experimental design according to Design of Experiments (DoE) was carried out in order to be able to investigate the influence of different influencing variables with reduced experimental effort. The experimental design carried out is shown in Table 2.

Table 2. Partial factorial experimental plan for milling trials based on DoE

Parameter set	Cutting speed v_c [m/min]	Feed per tooth f_z [mm]	Width of cut a_e [mm]	Feed direction in relation to AM build direction
1	30	0.03	1	perpendicular
2	45	0.045	1	perpendicular
3	30	0.045	1.5	perpendicular
4	45	0.03	1.5	perpendicular
5	45	0.03	1	parallel
6	30	0.045	1	parallel
7	30	0.03	1.5	parallel
8	45	0.045	1.5	parallel

This experimental plan was carried out successively for the three different relative densities (100 %, 84 %, 72 %). In the trials, the workpiece was machined line by line according to the specified process parameters. Flood cooling with Blaser Vasco 7000 was used. An Infinite Focus 5G, which measurement method is based on focus variation, and the associated EdgeMaster software from Alicona Imaging GmbH were used for the three-dimensional analysis of the surfaces. For the analysis of tool wear and chip shape, the VHX-6000 digital microscope from Keyence Corporation was utilized.

Electronic copy available at: https://ssrn.com/abstract=4259357

4. Results from milling trials

The results from the milling trials are presented in the following subsections. The results are divided according to the machinability criteria of tool life respectively tool wear, cutting force, surface finish and chip shape. The surface finish is actually not a significant criterion for roughing processes but is nevertheless considered here in order to record any noticeable effects after the porous material has been machined and to be able to better investigate the mechanisms involved.

4.1. Results from tool wear analysis

Under common cutting conditions cutting tools generally reach the end of their service life due to continuously increasing wear on the rake and flank faces. Wear is understood to be the progressive loss of material from the surface of a solid body, caused by mechanical causes. The main mechanisms causing tool wear are adhesion, abrasion, tribochemical reactions and surface disruption [10]. The cutting tool wear was analysed according to ISO 8688-2 [25] at certain feed travels l_f by taking microscopic images of all four cutting edges at the flank face and, for DoE analysis, averaging the four values for every tool.

Fig. 4 shows the microscopic images of the flank faces at different feed travels l_f for the three material porosities. From each of the four cutting edges, the one that was most representative for the other cutting edges was selected. For each material, the images are of the same cutting edge in different wear states. The process parameters are the lowest process parameters with the feed direction perpendicular to the AM build direction (parameter set 1, see table 2). The 100 % material exhibits uniform flank wear without any visible chipping. The 84 % and 72 % material, on the other hand, show sporadic, early chipping at the cutting edges that turns into a uniform chipping with increasing feed travel l_f.

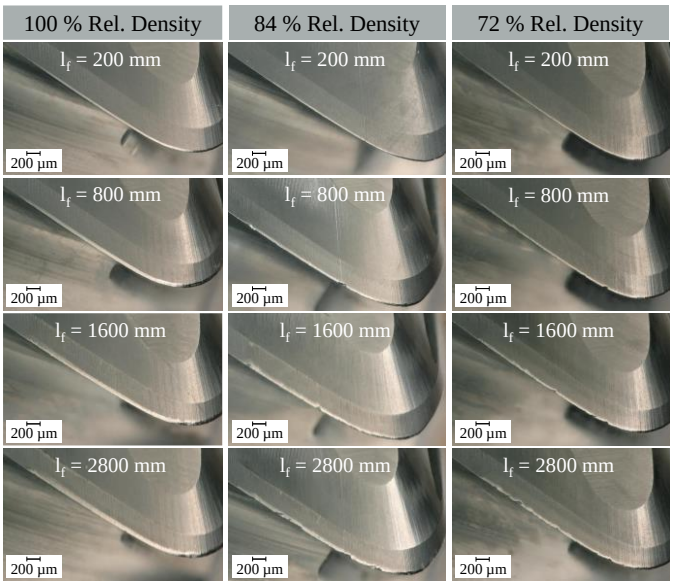

Fig. 4. Tool wear development at parameter set 1 (cf. table 2)

Fig. 5 shows the wear development at maximum process parameters and the feed direction parallel to the AM build direction. Even under these process conditions, the 100 % solid material exhibits uniform flank wear without visible chipping. This type of wear was observed in the investigations of the solid material for all parameter variants. It can therefore be concluded that the cutting tool and parameters are suitable for this AM solid material IN718, as it is the type of wear desired in the cutting process.

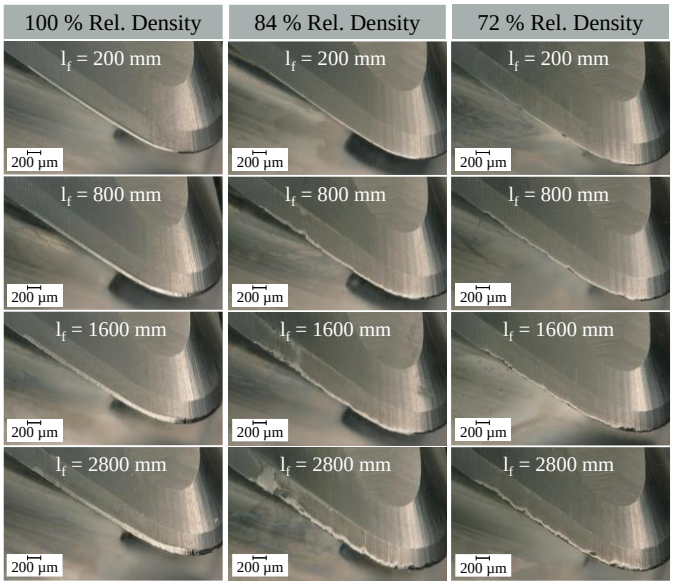

Fig. 5. Tool wear development at parameter set 8 (cf. table 2)

The two porous materials show, starting early, uniform chipping on the cutting edges with a tendency to higher, localized chipping at the position on the flanks adjacent to the work surface during cutting, which is typical for tool wear development [25]. This type of wear is not desired in the cutting process, since chipping occurs stochastically, and thus a prediction of tool life is generally not possible. Chipping occurred for the two porous materials for all parameter variations, so it can be concluded that the selected combination of tool and process parameters are not suitable for reliable machining of the porous material. It was noticeable that the 84 % material showed more severe chipping than the 72 % material.

A standardized way to quantify tool wear on the flank face is the width of the flank wear land VB [25]. This parameter is applicable as long as a continuously increasing flank wear without macroscopic chipping is present. However, if stochastic cutting edge breakouts dominate the wear pattern, VB is no longer applicable. Since at the beginning of the investigations mainly flank wear with only very few small chipping was present for all three material variations, the maximum width of the flank wear land VB_{max} for l_f = 200 mm could be evaluated according to DoE. The evaluation provides information about the initial wear of the cutting tools. Fig. 6 shows the main effect diagrams for VB_{max} after l_f = 200 mm. Due to the stochastic scattering of the tool wear and also the inaccuracies in the manual evaluation of the wear pattern, the results may only be evaluated as a rough tendency.

Electronic copy available at: https://ssrn.com/abstract=4259357

It is noticeable that the initial wear is lowest for the 72 % material and highest for the 100 % material. The 84 % material lies between the two. With regard to parameter variations, the trends of the three material variants differ slightly but, as mentioned earlier, these results should not be over-interpreted. The main finding is that the porous material initially has lower flank wear until chipping begins at the cutting edges and becomes the dominant wear form.

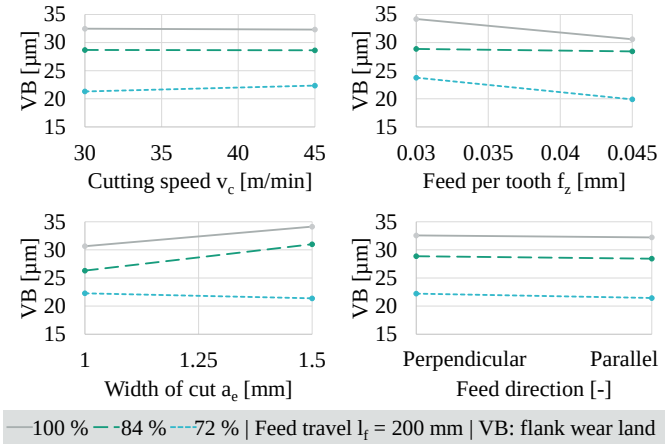

Fig. 6. Main effect diagrams for max. flank wear land VB_{max}

4.2. Results from cutting force analysis

The cutting force forms an assessment standard for the machinability of a material, since higher forces generally occur in materials that are difficult to machine. It is also a basis for determining the processes occurring at the location of chip formation and for explaining wear mechanisms [10]. According to DIN 6584, the cutting force generated during milling can be divided into two components, the active force F_a in the working plane and the passive force F_p perpendicular to the working plane. In this paper, only the active force is used for process evaluation, since its components generate the power during machining, while the passive force is not involved in this power [26]. The cutting force was continuously recorded during the trials with the force measuring platform at a sampling rate of 40 kHz. For evaluation, the signals of the individual, 40 mm long tool paths were separated, shortened by 10 % of signal length at the front and back and then the mean value was calculated. The mean values at certain feed travels l_f were then used for the DoE analysis. The main effects diagrams for the active force after l_f = 80 mm, so after only two lines on the workpiece, are shown in Fig. 7.

At this point, tool wear was very low, so its influence on the results was still negligible. Overall, it can be clearly seen that the active force is highest when milling the solid material and lowest for the 72 % material. The 84 % material is almost midway in between. Regarding the feed per tooth f_z and the width of cut a_e, all three porosities show the same tendency: a clear increase in active force with an increase of the process parameter. For increasing cutting speed v_c the 100 % and 84 % materials show a slight decrease of active force, whereas for the 72 % material the force is slightly increasing. When considering the feed direction, all variants exhibit somewhat higher active forces parallel to the AM build direction.

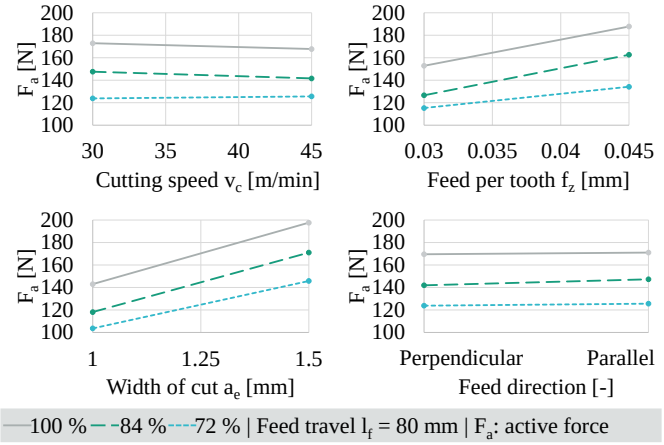

Fig. 7. Main effect diagrams for active force F_a

Fig. 8 shows the raw signals of the active force for the three material variants at a feed travel of l_f = 120 mm, i.e. with very low wear influence. Each peak is one tooth engagement of the milling tool. With increasing porosity, a stronger noise of the force signal can also be observed. Individual maximum values for the 72 % material are within the maximum force range of the 100 % material. However, the average value is significantly lower. The signals indicate that with the porous material there is a stronger mechanical alternating load, which is likely to accelerate tool wear.

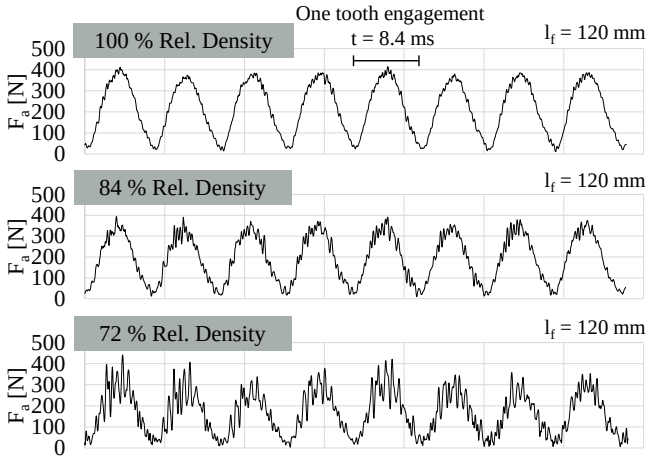

Fig. 8. Raw signal of active force F_a at parameter set 8 (cf. table 2)

4.3. Results from surface finish analysis

The analysis of the surface is not the main focus of this paper. The surface finish is not as relevant for roughing as it is for finishing. Nevertheless, it can contribute to the understanding of the process. Images of the milled surfaces, taken with the Alicona Infinite Focus 5G, are shown in Fig. 9, with the feed direction parallel (upper row) and perpendicular (lower row) to the AM build direction.

The porosity for the 84 % and 72 % material is clearly visible. While in the parallel direction the pores appear randomly distributed, in the perpendicular direction the

Electronic copy available at: https://ssrn.com/abstract=4259357

tendency towards a lattice structure can be seen. Compared to the initial state (cf. Fig. 2), the pores are clearly smeared up, indicating the presence of the ‘porosity closure phenomenon’.

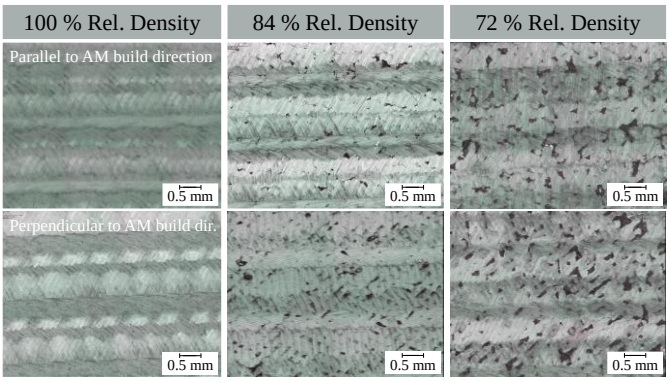

Fig. 9. Microscopic images of milled surfaces

4.4. Results from chip form analysis

Fig. 10 shows microscope images of representative chips for the three material variants at different process parameters. While the 100 % material delivers typical comma-shaped chips with a ‘closed’ surface, the two porous materials exhibit more irregular and disrupted surface structures with perforations. In particular, the chips of the 72 % material are heavily pitted.

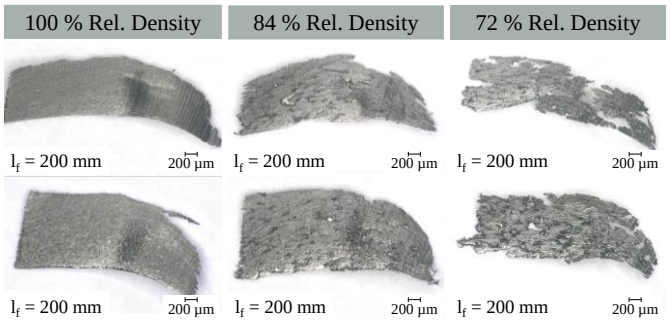

Fig. 10. Microscopic images of chips (upper row: parameter set 1, lower row: parameter set 8; cf. table 2)

5. Discussion

The milling trials with the three different material specifications showed some interesting tendencies for the described experimental setup. With regard to tool wear, the 100 % material exhibits uniform flank wear, but the porous variants show early starting uniform chipping (Fig. 4 & 5) with a tendency to higher, localized chipping at the position on the flanks adjacent to the work surface during cutting. It can be assumed that the alternating load on the cutting edge leads to the chipping and thus the 'interrupted cutting theory' may be applicable here. Even though the 'porosity closure phenomenon' can be observed in the microscopic images of the surfaces (Fig. 9), the pores are partially closed, but far from completely. The images of the chips also show a strongly disrupted surface (Fig. 10), so that the dominance of the 'deformed cutting theory' and thus the cutting of the cutting edge through compacted, ‘solid’ material seems rather unlikely here. The raw signal of the active force supports this hypothesis, since the porous material exhibits significantly higher oscillations in the force signal during one tooth engagement (Fig. 8) and thus the mechanical alternating load is higher. When evaluating the initial tool wear after a few tool paths (Fig. 6), it was found that initially there is only uniform flank wear for all three material variants and that this wear decreases with increasing porosity. It is assumed that the flank wear is lower than for the solid material due to the lower forces and the lower volume to be machined due to the porosity. However, because of the described load on the cutting edges in the porous material, chipping quickly becomes the dominant type of wear.

The general observation that, when machining porous material, the cutting force decreases as the porosity increases, but the machinability in terms of tool wear deteriorates [19], was also confirmed in these investigations. The lower forces result from the lower forming work required to deform the porous material, which has significantly lower strength values (see Table 2) [21]. Why the 84 % material shows more severe chipping than the 72 % material cannot be clearly explained. Since the two porous variants are two different materials with different LPBF process parameters, it cannot necessarily be assumed that there are clear trends with increasing or decreasing porosity. Further investigations are necessary to explain this observation.

6. Conclusion and Future Work

Compared to conventional manufacturing technologies, additive manufacturing (AM) offers several advantages. AM is increasingly coming into focus in aerospace and turbomachinery engineering, in particular the Laser Powder Bed Fusion (LPBF) process, also known as Selective Laser Melting (SLM). Depending on the component geometry, additive manufacturing requires support structures, which then usually must be removed by machining. Among others, the use of material with specifically induced porosity is suitable as a support structure. Compared to conventional support structures, a porous volume support ensures good heat dissipation in the LPBF process and thus homogeneous component properties, high holding forces and short process times. However, the machinability of porous, additively manufactured material has hardly been researched to date.

Inconel 718 (IN718) is the most widely used and most researched material among the high-temperature nickel alloys, which are applied in turbomachinery applications, for example. For this reason, this paper presents the results of machinability studies in milling porous AM IN718 with different relative densities (100%, 84%, 72%). The active force, milling tool wear, surface finish of the material after milling, and the resulting chip shape were investigated. As documented in numerous literature sources for machining porous powder metallurgy (PM) material, a decrease in cutting force combined with a deterioration in machinability in terms of tool wear was observed with increasing porosity. While the 100 % relative density material exhibited uniform flank wear, the milling of the two porous materials was dominated by uniform chipping with a tendency to higher, localized chipping at the position on

Electronic copy available at: https://ssrn.com/abstract=4259357

the flanks adjacent to the work surface during cutting. The reason for the chipping is seen in the strongly alternating load on individual cutting edge areas as they enter and exit the pores. This is said to cause microfractures and stronger vibrations, which strongly accelerate tool wear. A comparison of the active force curves for the three material variants confirms this hypothesis. The higher the porosity, the greater the oscillations in the force signal during one tooth engagement. Also consistent with the hypothesis, the chips of the porous materials have a disrupted structure with perforations.

Evaluating the initial tool wear after a few tool paths, it was found that initially there is only uniform flank wear for all three material variants and that this wear decreases with increasing porosity. It is assumed that the flank wear is lower than for the solid material due to the lower forces and the lower volume to be machined due to the porosity. However, because of the described stress on the cutting edge in the porous material, chipping quickly becomes the dominant type of wear. The 84 % material showed even more severe chipping than the 72 % material. The reason for this must be clarified in future investigations but could be due to the individual LPBF process parameters of the two materials.

A general recommendation regarding suitable process parameters for the machining of the porous AM IN718 cannot be made based on the presented results. Chipping was found to be the dominant type of wear for all process parameters investigated. Due to the stochastic behaviour of chipping, it is difficult to make tool life predictions and thus implement safe, industrially applicable processes. In future studies, it must be investigated whether the machining process can be optimized so that predominantly flank wear is present, such as by selecting a tougher carbide substrate or an optimized symmetrical or asymmetrical preparation of the cutting edge, for example by means of brushing [27]. The process vibrations and the microstructural properties of the milled rim zone should also be studied in more detail in order to better understand the mechanisms at work in the process.

Acknowledgements

The authors would like to thank the German Federal Ministry of Economic Affairs and Climate Action (BMWK) for the funding of the depicted research within the project AMB2S (20T1925H). The project was carried out within the framework of the funding program ‘LuFo VI-1’.

References

[1] Blakey-Milner, B., Gradl, P., Snedden, G., Brooks, M., Pitot, J., Lopez, E., Leary, M., Berto, F. & du Plessis, A. (2021). Metal additive manufacturing in aerospace: A review. Materials & Design, 209, 110008.
[2] DIN German Institute for Standardization (2003). DIN 8580 Manufacturing processes - Terms and definitions, division (DIN 8580:2003-09).
[3] Gu, D. (2015). Laser additive manufacturing of high-performance materials. Springer.
[4] Gibson, I., Rosen, D. W., Stucker, B., Khorasani, M., Rosen, D., Stucker, B., & Khorasani, M. (2021). Additive manufacturing technologies (Vol. 17). Cham, Switzerland: Springer.
[5] Schleifenbaum, H., Meiners, W., Wissenbach, K., & Hinke, C. (2010). Individualized production by means of high power Selective Laser Melting. CIRP Journal of manufacturing science and technology, 2(3), 161-169.
[6] Yap, C. Y., Chua, C. K., Dong, Z. L., Liu, Z. H., Zhang, D. Q., Loh, L. E., & Sing, S. L. (2015). Review of selective laser melting: Materials and applications. Applied physics reviews, 2(4), 041101.
[7] Ewald, S., Kies, F., Hermsen, S., Voshage, M., Haase, C., & Schleifenbaum, J. H. (2019). Rapid alloy development of extremely high-alloyed metals using powder blends in laser powder bed fusion. Materials, 12(10), 1706.
[8] Hebert, R. J. (2016). Metallurgical aspects of powder bed metal additive manufacturing. Journal of Materials Science, 51(3), 1165-1175.
[9] Grund, M. (2015). Implementierung von schichtadditiven Fertigungsverfahren: mit Fallbeispielen aus der Luftfahrtindustrie und Medizintechnik. Springer-Verlag.
[10] Klocke, F. (2018). Fertigungsverfahren 1: Zerspanung mit geometrisch bestimmter Schneide. Springer-Verlag.
[11] DIN German Institute for Standardization (2003). DIN 8589-3 Manufacturing processes chip removal - Part 3: Milling; Classification, subdivision, terms and definitions (DIN 8589-3:2003-09).
[12] Denkena, B., & Tönshoff, H. K. (2011). Spanen: Grundlagen. Springer.
[13] Yin, Q., Liu, Z., Wang, B., Song, Q., & Cai, Y. (2020). Recent progress of machinability and surface integrity for mechanical machining Inconel 718: a review. The International Journal of Advanced Manufacturing Technology, 109(1), 215-245.
[14] Hosseini, E., & Popovich, V. A. (2019). A review of mechanical properties of additively manufactured Inconel 718. Additive Manufacturing, 30, 100877.
[15] De Bartolomeis, A., Newman, S. T., Jawahir, I. S., Biermann, D., & Shokrani, A. (2021). Future research directions in the machining of Inconel 718. Journal of Materials Processing Technology, 297, 117260.
[16] Khanna, N., Zadafiya, K., Patel, T., Kaynak, Y., Rashid, R. A. R., & Vafadar, A. (2021). Review on machining of additively manufactured nickel and titanium alloys. Journal of Materials Research and Technology, 15, 3192-3221.
[17] Valdez, M., Kozuch, C., Faierson, E. J., & Jasiuk, I. (2017). Induced porosity in Super Alloy 718 through the laser additive manufacturing process: Microstructure and mechanical properties. Journal of Alloys and Compounds, 725, 757-764.
[18] Wood, P., Díaz-Álvarez, A., Díaz-Álvarez, J., Miguélez, M. H., Rusinek, A., Gunputh, U. F. & Płatek, P. (2020). Machinability of INCONEL718 Alloy with a Porous Microstructure Produced by Laser Melting Powder Bed Fusion at Higher Energy Densities. Materials, 13(24), 5730.
[19] Tutunea-Fatan, O. R., Fakhri, M. A., & Bordatchev, E. V. (2011). Porosity and cutting forces: from macroscale to microscale machining correlations. Proceedings of the Institution of Mechanical Engineers, Part B: Journal of Engineering Manufacture, 225(5), 619-630.
[20] Šalak, A., Selecká, M., & Danninger, H. (2005). Machinability of powder metallurgy steels. Cambridge Int Science Publishing.
[21] Benner, A., & Beiss, P. (2003). Zerspanung warmkompaktierter Sinterstähle im Grün- und Sinterzustand (No. RWTH-CONV-120982). Fakultät für Maschinenwesen.
[22] Hu, B., Warzel, R., Ropar, S., & Neilan, A. (2017). The effect of porosity on machinability of PM materials. International Journal of Powder Metallurgy, 53(1), 27-36.
[23] Kurt, A., & Ates, H. (2007). Effect of porosity on thermal conductivity of powder metal materials. Materials & design, 28(1), 230-233.
[24] British Standards Institution (2019). ISO 6892-1 Metallic materials. Tensile testing. Method of test at room temperature (BS EN ISO 6892-1:2019).
[25] ISO International Organization for Standardization (1989). ISO 8688-2 Tool life testing in milling; part 2: end milling (ISO 8688-2:1989-05).
[26] DIN German Institute for Standardization (1982). DIN 6584 Terms of the cutting technique; forces, energy, work, power (DIN 6584:1982-10).
[27] Bergs, T., Schneider, S. A. M., Amara, M., & Ganser, P. (2020). Preparation of symmetrical and asymmetrical cutting edges on solid cutting tools using brushing tools with filament-integrated diamond grits. Procedia CIRP, 93, 873-878.
[28] Kelliger, T., Schraknepper, D., Bergs, T. (2021). Fundamental Investigations on the Machinability of Additively Manufactured Multi-Materials. MM Science journal, 5, 5098-5105.

Electronic copy available at: https://ssrn.com/abstract=4259357